Adaptive VMD and PSO-MOMEDA Algorithm based method for Rotor System Fault Diagnosis

Fengfeng Bie[*], Ying Zhang, Fengxia Lyu, Xingting Miao, Yifan Wu

School of Mechanical Engineering, Changzhou University, Changzhou, Jiangsu, China 213016

*Corresponding author.

Abstract

In this paper, a fault diagnosis method combining the variational mode decomposition (VMD) with adaptive parameters and multi-point optimal minimum entropy deconvolution adjusted (MOMEDA) optimized by partial swarm optimization algorithm (PSO) aiming at the problem that the fault information is hard to extract from the overwhelmed vibration signal when the rotor system works in strong noise setting is proposed. Firstly, the original signal is decomposed into intrinsic mode components (IMF) series by VMD, from which the specified IMF components are selected for signal reconstruction according to the correlation coefficient – kurtosis criterion, and then the reconstructed signal is processed with the MOMEDA model for the filtering. Finally, the rotor system fault type is identified through the signal envelope spectrum analysis. Simulation test and rotor fault experiments results show that the improved VMD model with PSO-MOMEDA method can primely remove the noise from the vibration signal of the rotor system and accomplish the fault mode recognition with avoiding the blind selection of parameters in the process.

Keywords: Rotor System, Variational Mode Decomposition, Multi-point Optimal Minimum Entropy Deconvolution Adjusted, Particle Swarm Optimization Algorithm, Fault Diagnosis.

I. Introduction

With the continuous development of industrialization, rotating machinery has been widely used, accounting for about 80% of the total amount of mechanical equipment. The core components, rotor and support system, generally play the important role of bearing and transferring load, and their running status directly affects the performance of the whole equipment. According to statistics, about 60% of the rotating machinery failure are caused by the rotor system failure. However, the regular disassembly and inspection will not only cause human resources wastes, but also renders damage to the parts in the rotor system, and delay the normal production activities in the actual industrial production. Therefore, it is particularly vital to ensure the safe and reliable operation of rotating machinery by collecting and analyzing the vibration signals of the rotor system in real time. At present, extracting the impact components from the signal and analyzing the spectrum is the most commonly used analysis method to figure out the feature frequency of the fault so as to determine the type of fault [1,2]. As the outward transmission process of impact signal can be seen as a linear convolution process of shock signal and transmission channel, and the extraction of shock components from the original signal can be treated as deconvolution [3]. MOMEDA is a novel deconvolution method proposed by Mcdonald et al. [4], which overcomes the disadvantages that the minimum entropy deconvolution (MED) cannot reflect the true situation of faults and maximum correlated kurtosis deconvolution (MCKD) parameters selection is difficult [5,6]. However, due to the large amount of noise mixed in the original vibration signal, the fault characteristic frequency spectrum in its envelope spectrum is not obvious if the signal is deconvoluted directly by MOMEDA, therefore it is usually preprocessed with noise reduction first. Empirical mode decomposition (EMD), local mean decomposition (LMD), wavelet transform threshold denoising and other methods [7-10] are all methods for processing nonlinear and non-stationary signals. In recent research, scholars have executed on the difference among EMD and LMD, both of which could decompose the original signal

into the sum of multiple components, but there are serious problems such as modal aliasing and endpoint effect [11,12]. Wavelet transform threshold denoising is a commonly used noise reduction algorithm in practical engineering, which achieves denoising by selecting an appropriate threshold function while preserving as many features of the original signal as possible [13]. Since there are many parameters in the threshold function that affect the denoising performance, reasonable selection of parameters is required. VMD is used to decompose the signal by introducing variational constraint, which surmounts the issues of modal aliasing and endpoint effect, and requires few parameters to be set, thus it is extensively applied for noise suppression of vibration signals [14].

This paper proposes a method that combined improved VMD with PSO-MOMEDA based on the problem that the faulty characteristics of the rotor system vibration signals are not easily extracted in the strong noise background. Since the kurtosis (Ku) can represent the degree of shock in the signal and the relative entropy (KL) [15-17] can represent the degree of irregularity of the system and the degree of similarity of two probability distributions, this paper proposes a new integrated index Z (Z=Ku/KL) based on two indicators, kurtosis and relative entropy, to obtain the maximum Z and thus determine the optimal parameters K, α and L in the method.

This article is organized as follows, theoretical background of VMD and MOMEDA, the process of parameter optimization and the steps based on VMD with adaptive parameters and PSO-MOMEDA are discussed in Section 2. A fault simulation signal of bearing inner ring is established in Section 3, and the fault feature frequency is obtained by using the proposed method and its type is identified. Experimental verification is carried out in Section 4, where the validity of the proposed method is certificated by processing the single and couple signals that measured in the experiment. Finally, the conclusions are drawn in Section 5.

II. Principle and methods

2.1 VMD

VMD is an adaptive decomposition method that searches the optimal variational model through multiple iterations, where the original vibration signal $x(t)$ to be analyzed is composed of several IMF components, each of which can be regarded as an AM-FM signal:

$$u_k(t) = A_k(t)\cos(\phi_k(t)) \tag{1}$$

where $A_k(t)$ is the instantaneous amplitude of $u_k(t)$, $\phi_k(t)$ is the phase of $u_k(t)$.

According to the minimum sum of the frequency band width of each component, the constraint condition is that the result of the addition of each component is the original signal, the constraint equation of the variational mode decomposition is:

$$\left\{ \min_{\{u_k\}\{w_k\}} \left\{ \sum_k \left\| \partial_t \left[\left(\delta(t) + \frac{j}{\pi t} \right) * u_k(t) \right] e^{-jw_k(t)} \right\|_2^2 \right\} \atop s.t. \quad \sum u_k = x(t) \right. \tag{2}$$

where $\{u_k\}$ is the modal components of the decomposed original signal, $\{w_k\} = d\{\phi_k(t)\}/dt$ is the central frequency corresponding to each IMF components, ∂_t is the partial derivative of t, $\delta(t)$ is the delta function.

In order to fetch the optimal solution of Eq. (2), the penalty factor α and the Lagrange multiplier λ are introduced to make the solution model become unconstrained model:

$$L\left(\{u_k\},\{w_k\},\lambda\right)=$$

$$\alpha\sum_{k=1}^{K}\left\|\left[\partial_t\left[\delta(t)+\frac{j}{\pi t}\right]*u_k(t)\right]e^{-jw_kt}\right\|_2^2$$

$$+\left\|x(t)-\sum_{k=1}^{K}u_k(t)\right\|_2^2+\left\langle\lambda(t),x(t)-\sum_{k=1}^{K}u_k(t)\right\rangle$$

(3)

where $\lambda(t)$ is the Lagrange multiplier, α is the quadratic factor, $\langle\ \rangle$ is the inner product.

The specific algorithm steps are as follows:

Step 1: Initialization $\{\hat{u}_k^1\}$, $\{w_k^1\}$, $\hat{\lambda}^1$, n←0;

Step 2: n←n+1, and updated $\hat{u}_k$, w_k according to Eq. (3):

$$\begin{cases}\hat{u}_k^{n+1}(w)=\dfrac{\hat{x}(w)-\sum_{i<k}\hat{u}_i^{n+1}(w)-\sum_{i>k}\hat{u}_i^n(w)+\dfrac{\hat{\lambda}^n(w)}{2}}{1+2\alpha\left(w-w_k^n\right)^2}\\[20pt]w_k^{n+1}=\dfrac{\int_0^\infty w\left|\hat{u}_k^{n+1}(w)\right|^2dw}{\int_0^\infty\left|\hat{u}_k^{n+1}(w)\right|^2dw}\end{cases}$$

(4)

Step 3: Update λ :

$$\hat{\lambda}^{n+1}(\omega)\leftarrow\hat{\lambda}^n(\omega)+\tau\left[\hat{x}(\omega)-\sum_K\hat{u}_K^{n+1}(\omega)\right]$$

(5)

Repeat steps 2 and 3 until satisfied $\sum_i\left\|\hat{u}_i^{n+1}-\hat{u}_i^n\right\|_2^2/\left\|\hat{u}_i^n\right\|_2^2<\varepsilon$ that the iteration is completed and K modal components are output.

2.2 MOMEDA

The fault vibration signal is assumed to be:

$$m=e*n+s$$

(6)

where m is the measured signal, n is the system impact signal, e is the transfer function of the system, and s is stochastic noise.

The main principle of the MOMEDA algorithm is to identify the inverse fold product for a multi-pulse target whose position is known, and to find a filter that maximizes the return of m to n, i.e.

$$m = f * n = \sum_{p=1}^{N-L} f_p m_{p+L-1} \qquad (7)$$

where $p = 1, 2, \cdots, N-L$.

The objective function is described as:

$$MOMEDA(n,q) = \max_{f} \frac{q \cdot n}{\|n\|} \qquad (8)$$

where q is the objective vector that defines the position and weight of the deconvolution target impact component. Deconvolution works best when q fits perfectly with n, and the corresponding filter is the best filter f.

The solution of Eq. (8) is equivalent to solving Eq. (9):

$$\frac{d}{df}\left(\frac{q^T n}{\|n\|}\right) = 0 \qquad (9)$$

where $f = f_1, f_2, f_3, \cdots, f_L, q = q_1, q_2, q_3, \cdots, q_{N-L}$.

Combining Eq. (7), Eq. (8) and Eq. (9), and making $\left[m_{p+L-1}, m_{p+L-2}, \cdots, m_p \right]^T = M_p$, we get:

$$
\begin{aligned}
\frac{d}{df}&\left(\frac{q^T n}{\|n\|}\right) \\
&= \|n\|^{-1}\left(q_1 M_1 + q_2 M_2 + \cdots + q_p M_p\right) \qquad (10) \\
&\quad - \|n\|^{-3} q^T n X_0 n = 0
\end{aligned}
$$

Let $X_0 = [M_1, M_2, \cdots, M_p]$, simplify the Eq. (10) to $\|n\|^{-1} X_0 q - \|n\|^{-3} q^T n X_0 n = 0$, and substitute $n = X_0^T f$ to obtain:

$$f = \left(X_0 X_0^T\right)^{-1} X_0 q \qquad (11)$$

The impact signal n can be recovered by substituting Eq. (11) to $n = X_0^T f$.

2.3 Parameter optimization and diagnosis process

This paper proposes a rotor system fault diagnosis method combining adaptive parameters VMD and PSO-MOMEDA, in which VMD involves the number of decomposition layers K and penalty factor α, and MOMEDA involves the filter length L. To avoid the subjectivity of artificial selection, the parameters in the algorithm are optimally selected with Z as the target function, and it is the best value when Z is maximum. The particle swarm size is set as 25, the learning factor c1=c2=2, the inertia weight w1=0.95, w2=0.4, the number of iterations is 50, and the range of L for the optimization search is [100,2000] in the particle swarm algorithm, Fig.1 shows the process, and the specific steps are as follows:

Step 1: The original signal is decomposed by VMD, and reconstructed by selecting the corresponding modal components in the light of the correlation coefficient(ρ)-kurtosis (ku) criterion.

Step 2: The reconstructed signal is processed with the MOMEDA model for filtering to obtain an enhanced signal and make envelope spectral of this signal to analyze.

Step 3: The characteristic frequency of the fault is compared with the envelope spectrogram of the enhanced signal to discern the fault type.

As the study processing, two main steps are included, i.e., the simulation analysis for the primarily validation of the adaptive VMD method and the further verification of the proposed entire VMD and PSO-MOMEDA model.
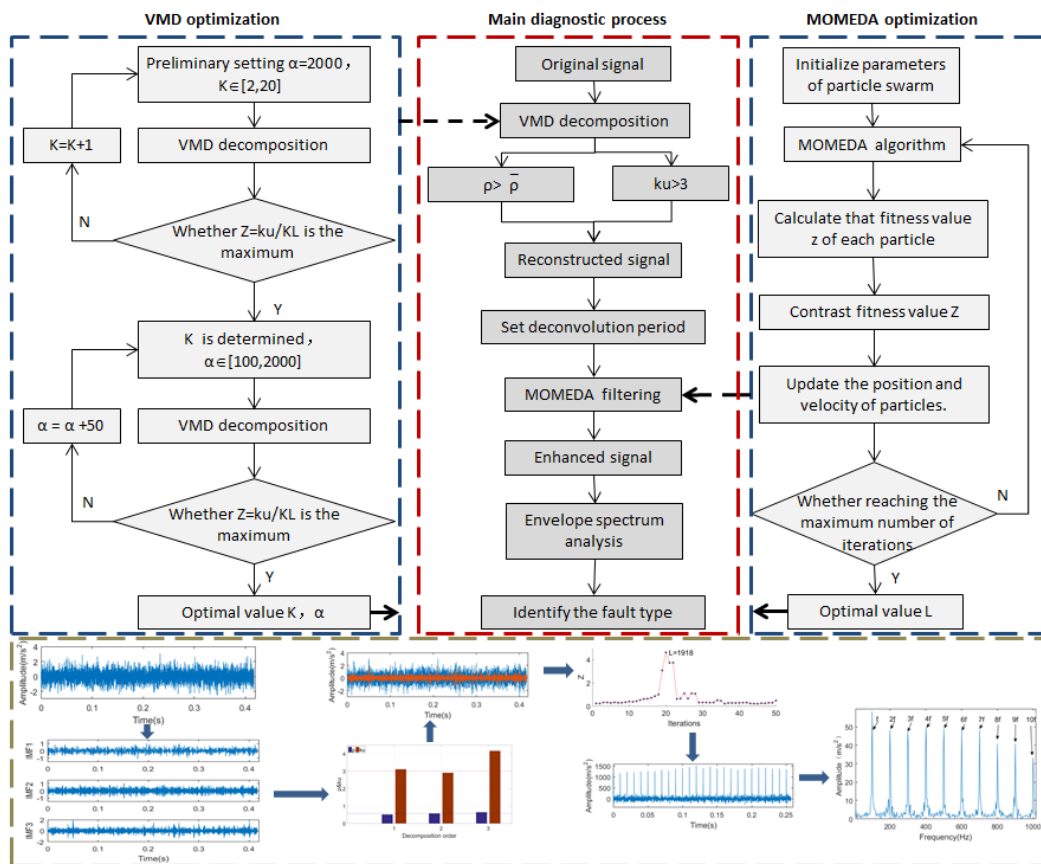
Fig 1: Parameter optimization and diagnosis flow chart

III. Simulation analysis

3.1 Simulation signal construction

A mathematical model of the vibration signal when the inner ring of rolling bearing fails in the rotor system is constructed in order to prove the effectiveness of this method [18]:

$$\begin{cases} y(t) = x(t) + n(t) = \sum_i A_i m(t - iT) + n(t) \\ m(t) = \exp(-Ct)\cos(2\pi f_n t) \\ A_i = 1 + A_0 \cos(2\pi f_r t) \end{cases} \qquad (12)$$

where $x(t)$ is the cyclic impact component, displacement constant A_0 is 0.5, resonance frequency f_n is 4kHz, rotation frequency f_r is 20Hz, attenuation coefficient C is 500, inner circle fault characteristic frequency f_i =1/T=100Hz, $n(t)$ is the Gaussian white noise component, sampling frequency f_s is 12kHz, and the number of sampling points is 5000.

In order to simulate the fault signal in real environment, Gaussian white noise of -10dB is added to the simulation signal of rolling bearing inner ring fault, Fig. 2 depicts the simulation signal after adding noise. From the figure that we can see the time domain waveform is complex, the shock is not obvious, and only the fundamental frequency of the fault can be noticed in the envelope spectrum, and there are more components of other interference frequencies.

(a) Time domain graph
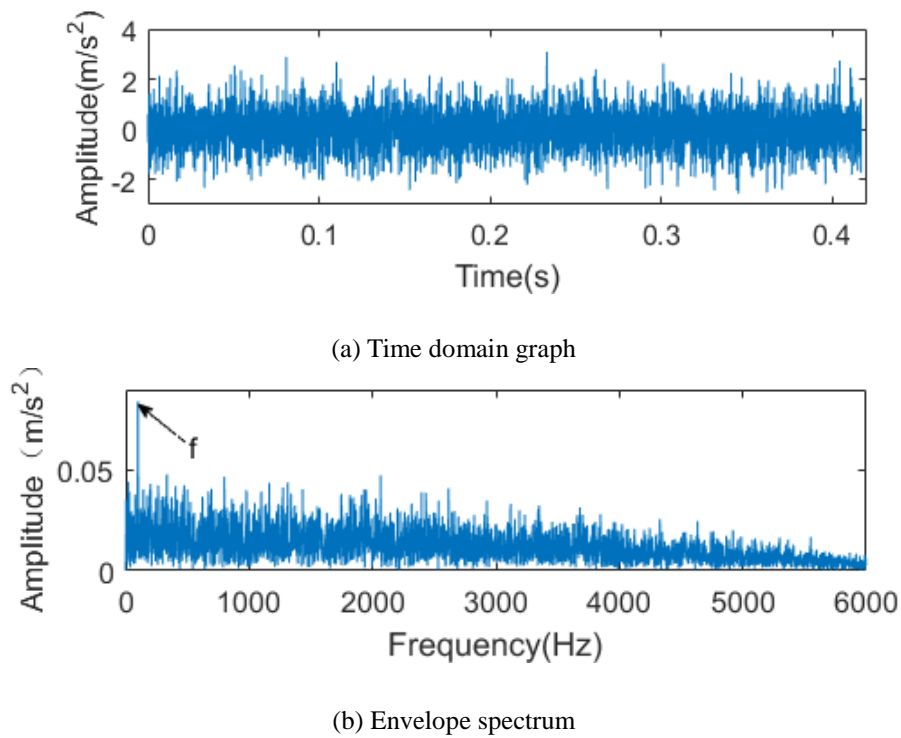
(b) Envelope spectrum
Fig 2: Time-frequency spectrograph of simulation signal

3.2 Simulation signal processing

According to the above method to determine K=3 and α=350, the three IMF components after decomposition are shown in Fig.3. The kurtosis and correlation coefficients of each component are calculated as shown in Fig.4.
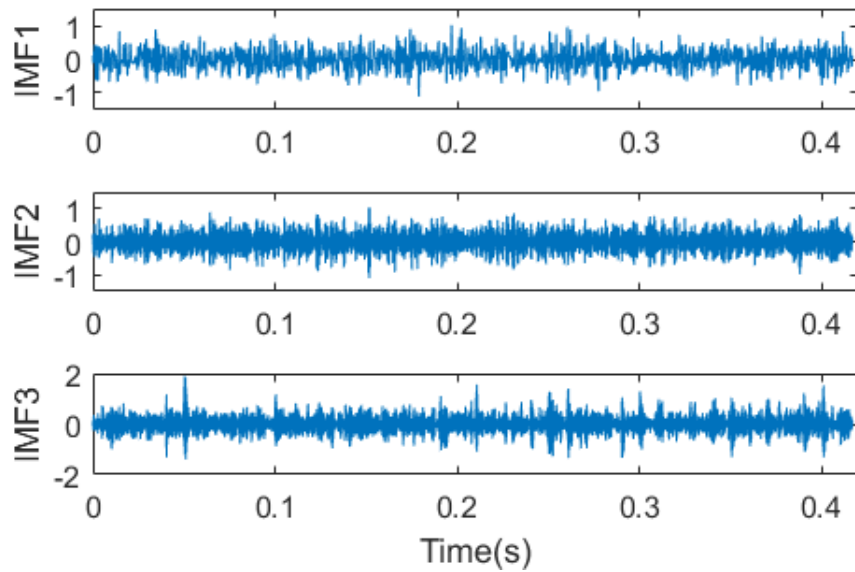
(a) Time domain graph
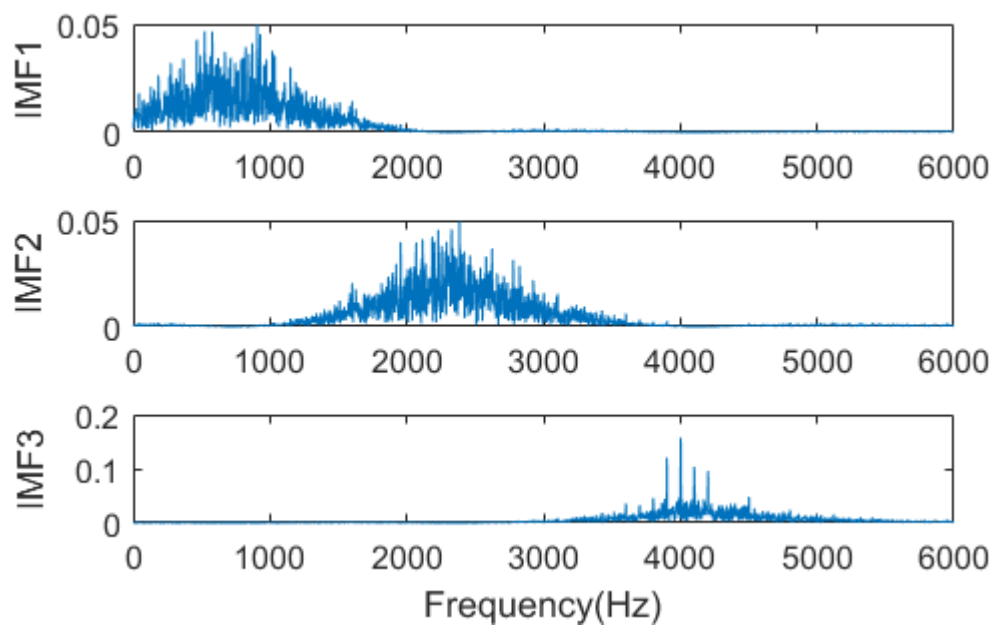
(b) Spectral graph
Fig 3: Results of VMD
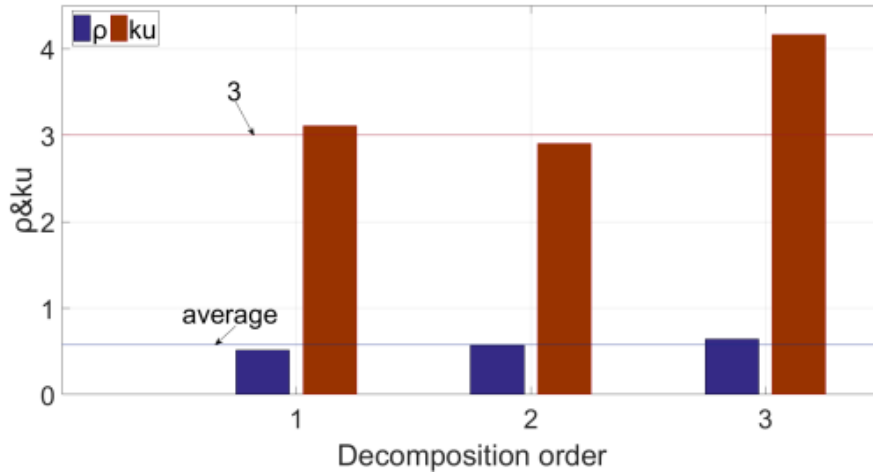
Fig 4: Component index chart

The correlation coefficient between IMF3 and the original signal is greater than the mean value and its kurtosis value is greater than 3 that can be perceived from Fig.4, which retains the most impact features in the original signal. From Fig.3b, it can be found out that each component is relatively independent and has not been hyper-decomposed, IMF3 well retains the components of medium-high frequency and reduced the interference of low frequency components, and can be seen from Fig. 5 that its temporal waveform shock is more obvious.
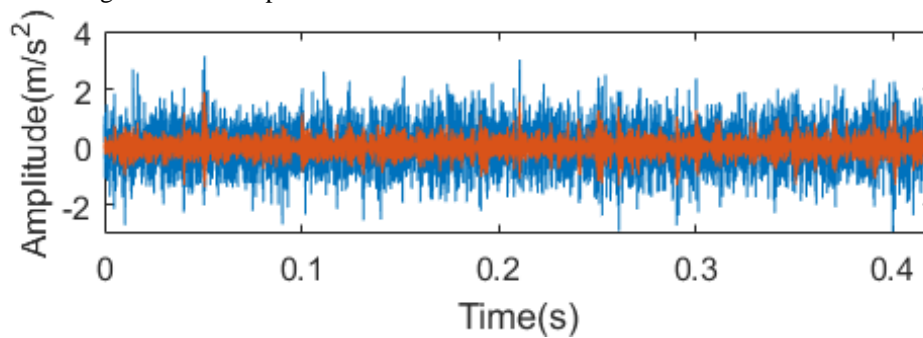
Fig 5: Comparison between reconstructed signal and original signal
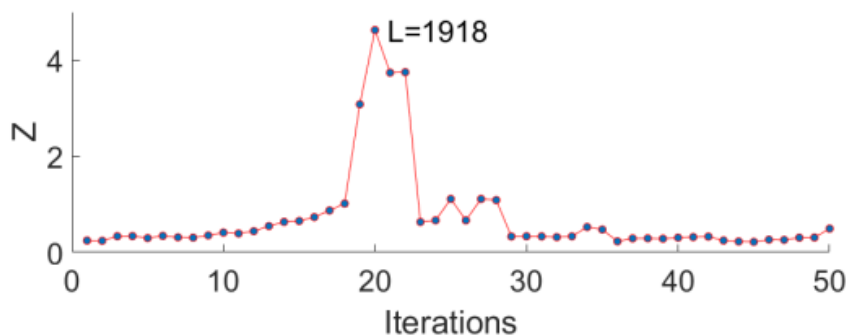
Fig 6: Curve of Z with the number of iterations

There are 50 iterations in total. It can be seen from Fig.6 that Z reach the maximum value and the filter order L is 1918 when the iterations reach the 20th time. MOMEDA deconvolution of IMF3 (L=1918, window function is [1918,1], period T is 120) is performed to obtain the temporal waveform, and the envelope spectrum analysis is

performed shown in Fig.7. The characteristic frequency and the frequency doublings are displayed in the Fig.7b, which indicates that the bearing inner ring of the rotor system has out of order and proving the significance of the method proposed in this paper.
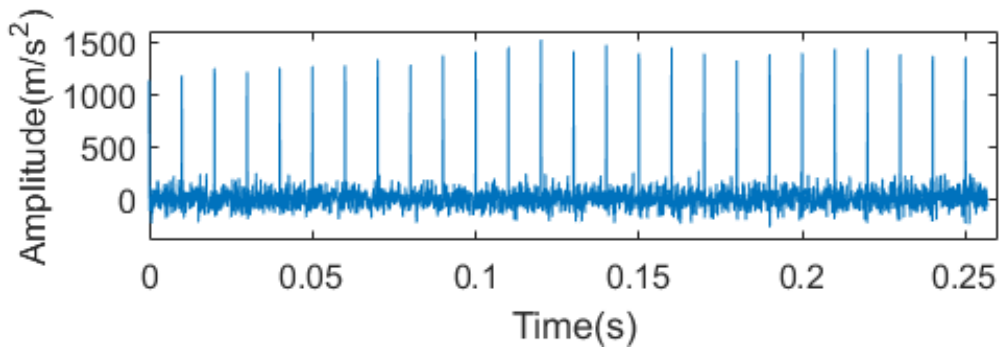
(a) Time domain graph
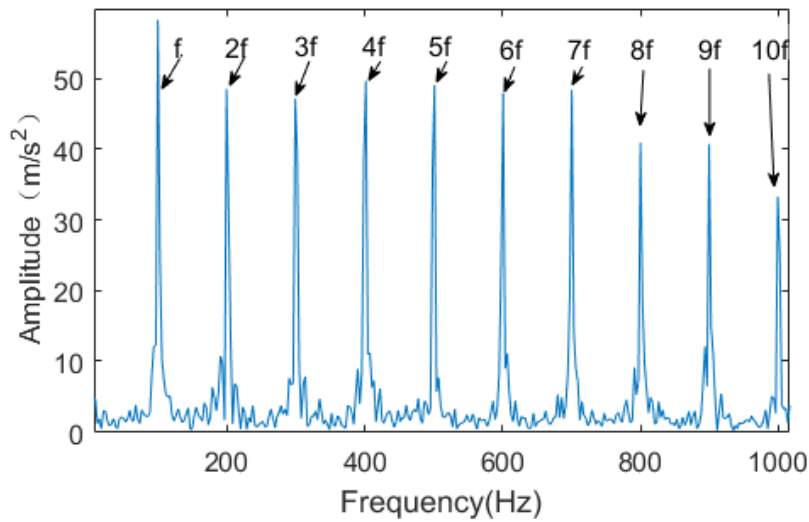
(b) Envelope spectrum

Fig 7: Temporal waveform and envelope spectrum of MOMEDA deconvolution reconstruction signal

IV. Experimental validation

To verify that the method is also useful on the actual measured rotor system signals, a rotor system fault simulation test bench was built to analyze the single fault of the outer ring and the composite fault of the outer ring and rotor imbalance, the test bench is shown in Fig. 8, and the data acquisition process is shown in Fig. 9.
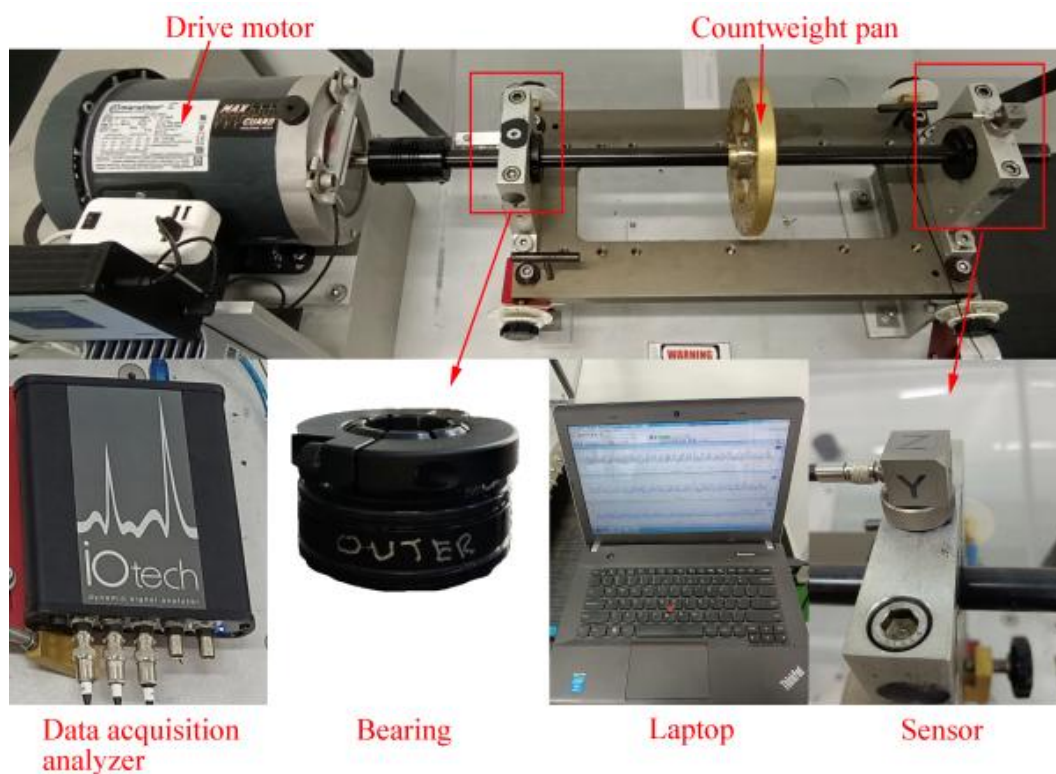
Fig 8: Test bench
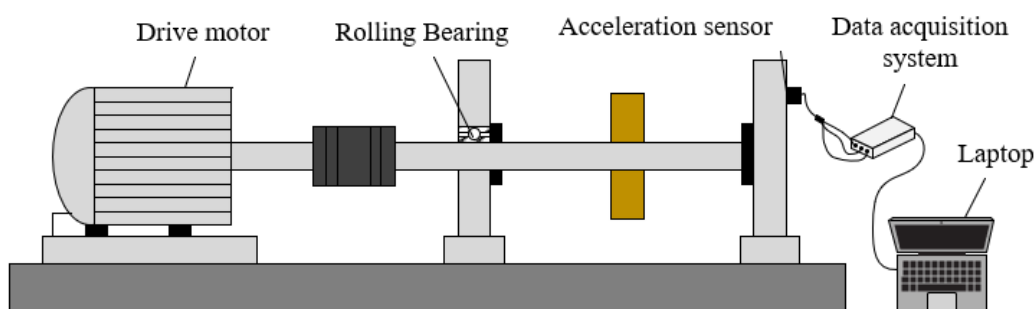
Fig 9: Data gathering process

The type of rolling bearing we used is MB ER-12K, and the fault is set in its outer ring, and the rotor unbalance fault is set by increasing the mass on the counterweight pan, and the sampling frequency is set as 12800Hz, the number of sampling points is 8000, and the shaft speed is 1200r/min in this experiment. The geometric parameters of the rolling bearing size are shown in Tab.1. The rotor unbalance fault characteristic frequency is 20Hz, and the inner ring fault characteristic frequency of the rolling bearing is calculated as 61.27Hz according to the rolling bearing fault characteristic frequency calculation formula [19].

TABLE I. Geometric parameters of rolling bearing

Geometric parameters	values
Number of rolling bodies	8
Rotational frequency	20Hz
Rolling body diameter	7.9375mm
Raceway section diameter	33.4772mm

Contact angle	9.08 °

4.1 Outer ring fault
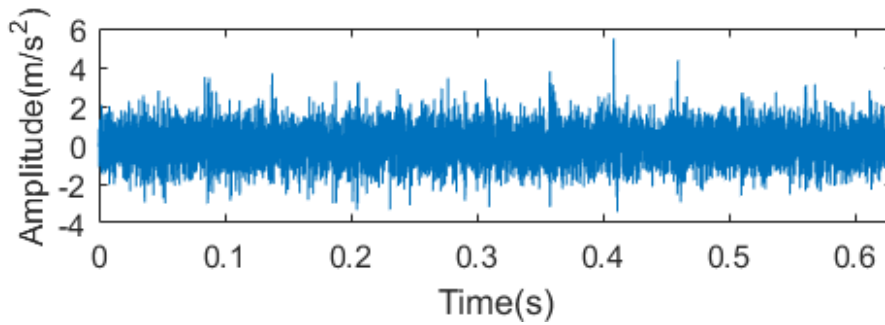
(a)   Time domain graph
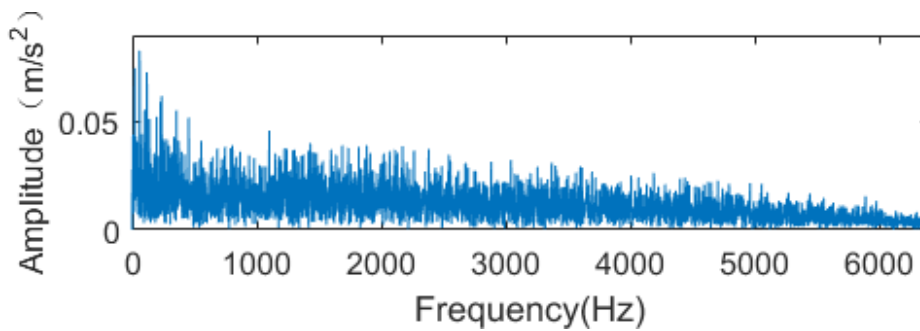
(b) Envelope spectrum
Fig 10: Time-frequency spectrograph of bearing outer ring fault

The time domain diagram and envelope spectrum of the vibration signal of rolling bearing outer ring fault measured in the experiment are shown in Fig.10, from which it can be seen that the temporal waveform is interfered, and the envelope spectrum contains disturbing components, which could not be beneficial for the fault mode determination. The acquired vibration signal is decomposed by adaptive VMD method, where K=6, α=1850, and the six IMF components after decomposition are shown in Fig.11. The results of calculating the kurtosis of the six IMF components and the correlation coefficient between them and the original signal are shown in Fig.12.
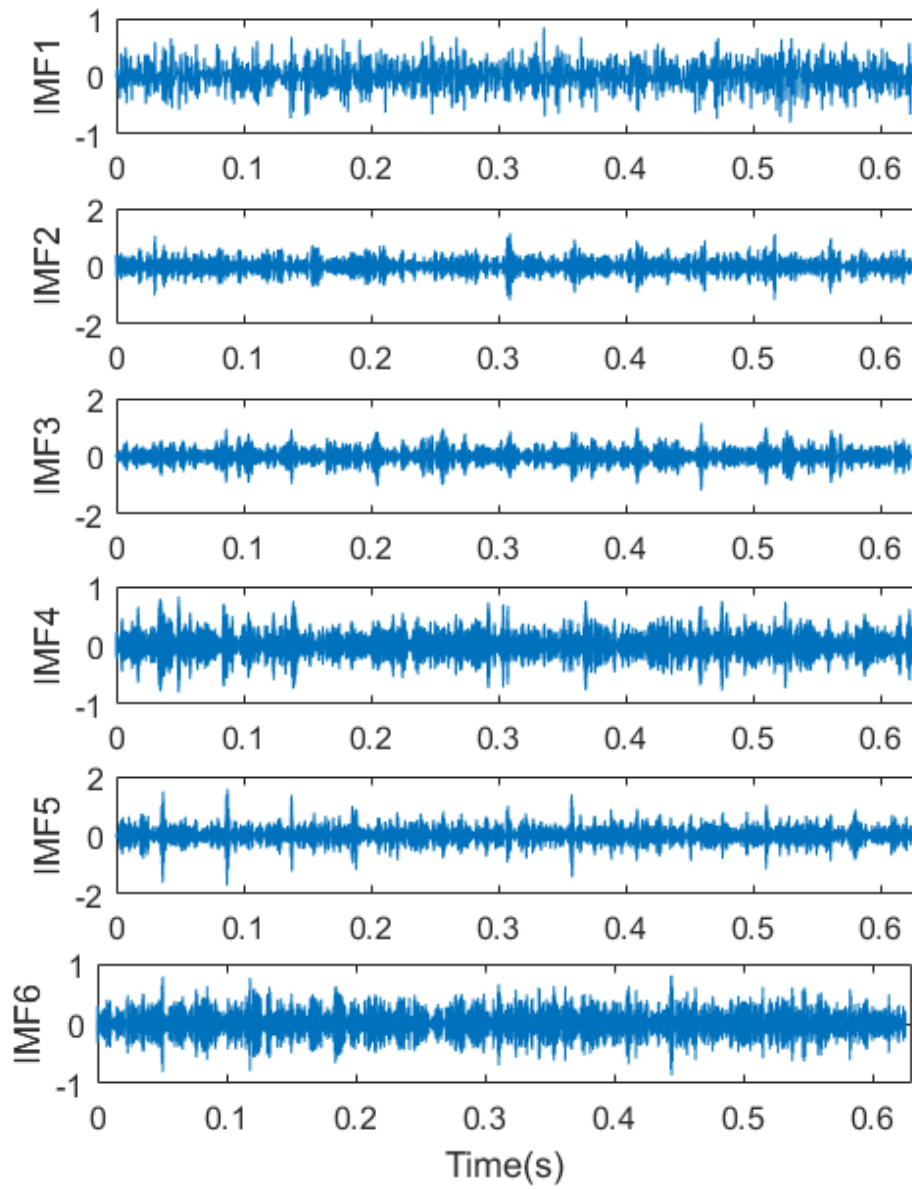
(b)   Time domain graph
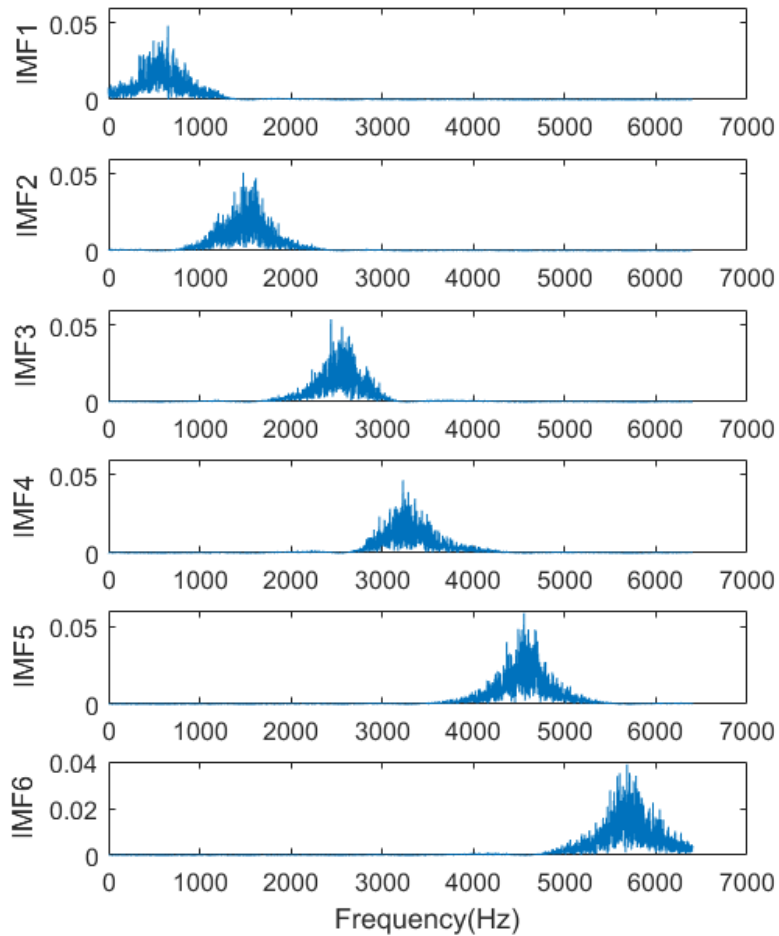
(b) Spectral graph
Fig 11: Results of VMD
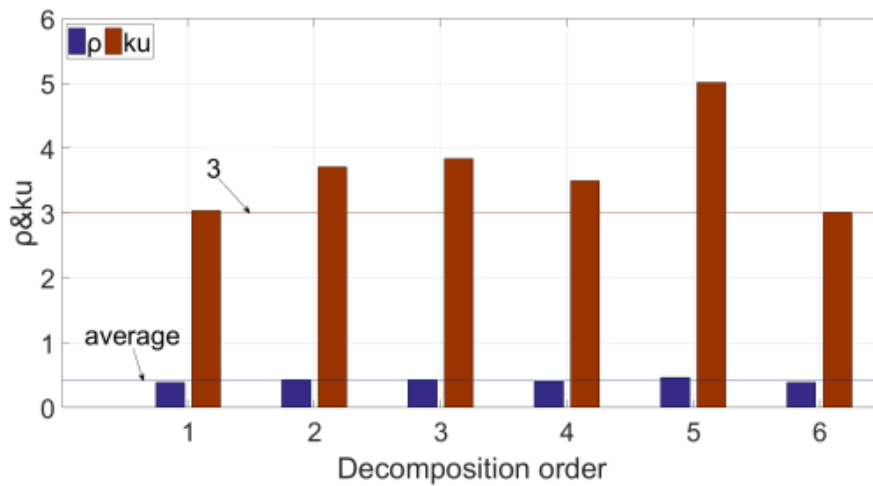
Fig 12: Component index chart

It could be observed from Fig. 11(b) that there is no hyper-decomposition phenomenon, According to Fig. 12, IMF2, IMF3 and IMF5 are selected for signal reconstruction. The reconstructed signal and the original signal is shown in Fig.13.
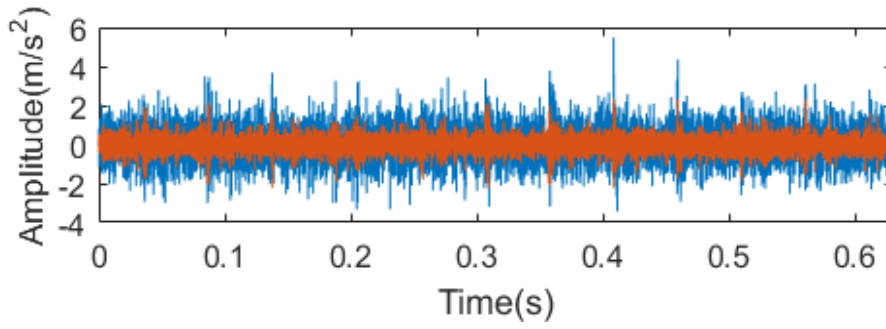
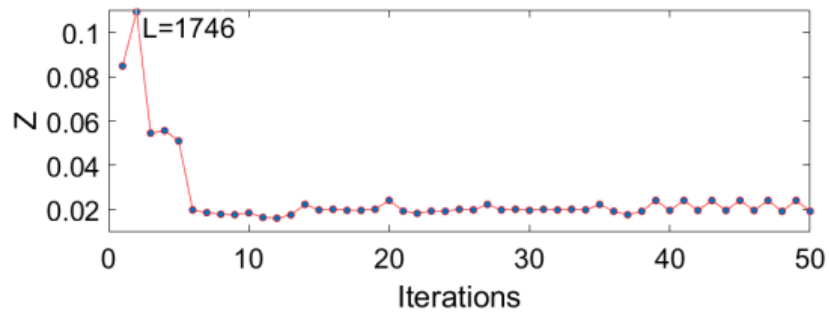Fig 13: Comparison between reconstructed signal and original signal

Fig 14: Curve of Z with the number of iterations

It can be seen from Fig.14 that when the iterations reach the 2th time, Z reach the maximum value and the filter order L was 1746. The reconstructed signal was deconvoluted by MOMEDA (L=1746, window function is [1746,1], period T is 208.91) to obtain the temporal waveform, and the envelope spectrum analysis was performed shown in Fig.15.
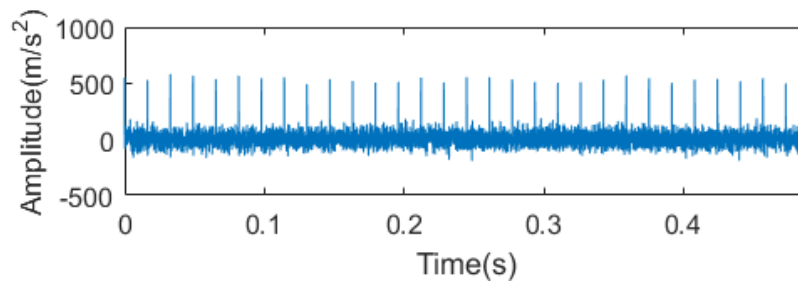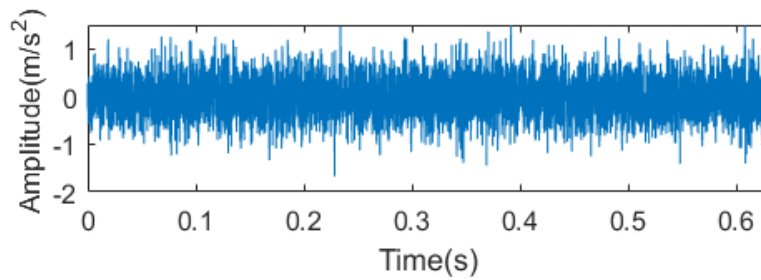

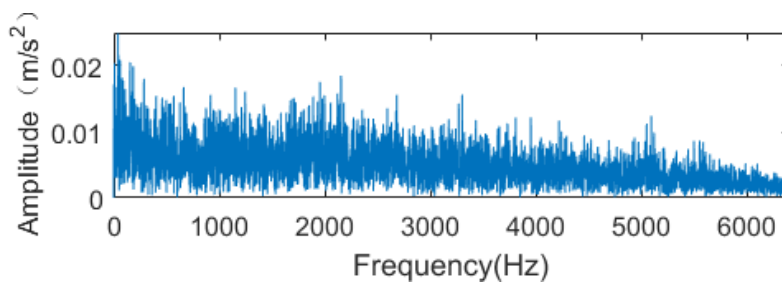(a)Time domain graph
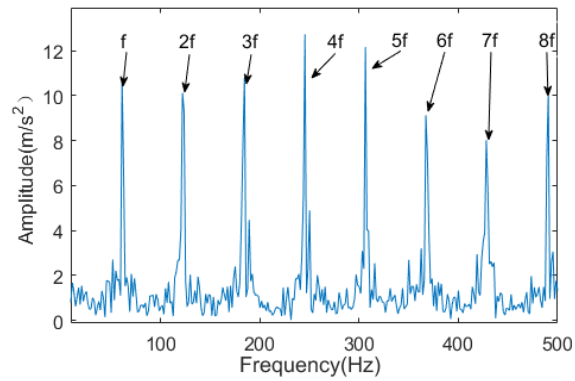
(b) Envelope spectrum

Fig 15: Temporal waveform and envelope spectrum of MOMEDA deconvolution reconstruction signal

From the envelope spectrum analysis, the characteristic frequency of bearing outer ring fault and their multiples could be obtained, which is consistent with the experimental fault type.

4.2 The composite fault of the outer ring and rotor imbalance


(a)Time domain graph

(b) Envelope spectrum

Fig 16: Time-frequency spectrograph of outer ring-rotor imbalance fault

As for the compound fault mode, the outer ring of rotor system and rotor imbalance are set in the experimental bench. Fig. 16 illustrates the time domain waveform diagram and envelope spectrum of the composite fault. The signal is decomposed primarily with VMD method (K=2, α=100), and Fig. 17 shows two IMF components after decomposition. The calculated kurtosis of these two IMF components and the correlation coefficient between them, together with the original signal are shown in Fig.18.
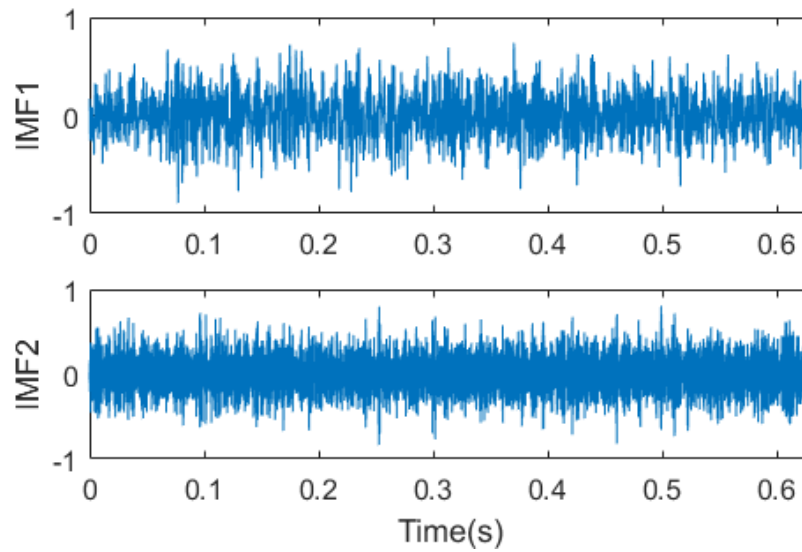
(a)Time domain graph
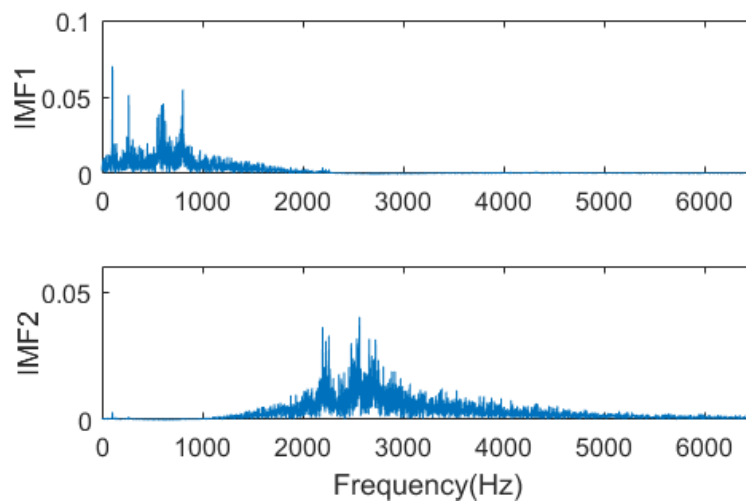
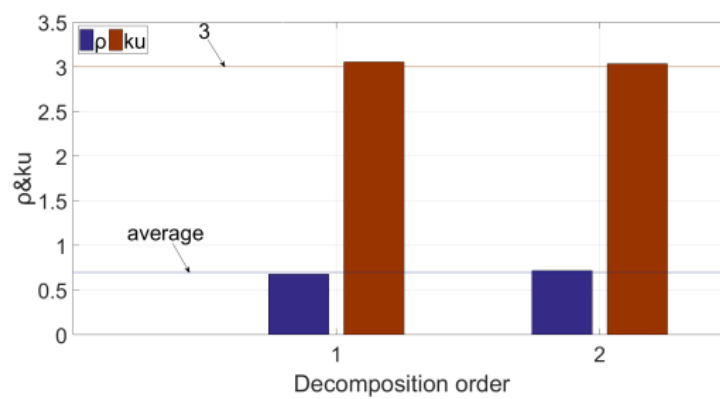(b) Spectral graph
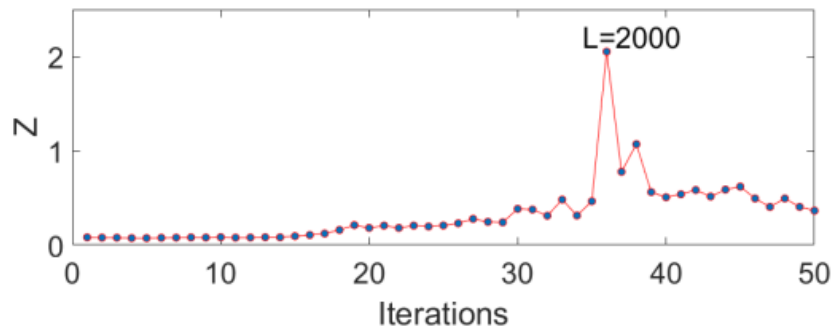Fig 17: Results of VMD
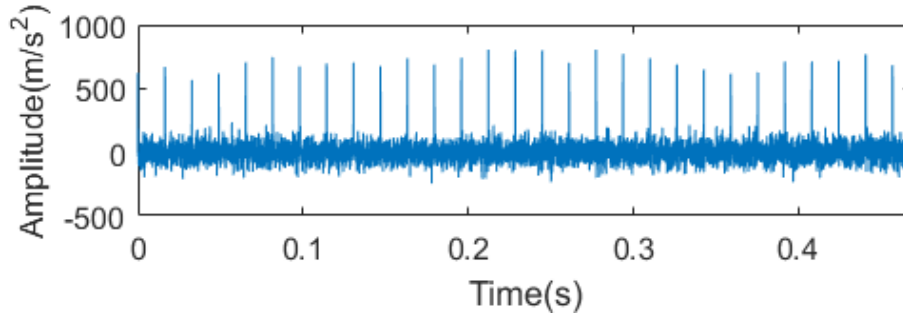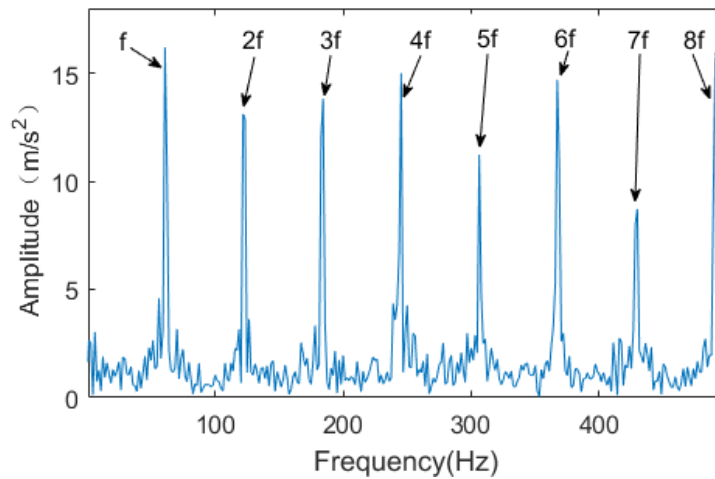

Fig 18: Component index chart

Fig 19: Curve of Z with the number of iterations (outer ring)

It can be seen from Fig. 18 and Fig.19 that IMF2 is selected for MOMEDA deconvolution with L=2000 when the period T is 208.91, and the window function is [2000, 1], and the temporal waveform shown in fig. 20 is obtained and analyzed by envelope.

(a)Time domain graph

(b) Envelope spectrum
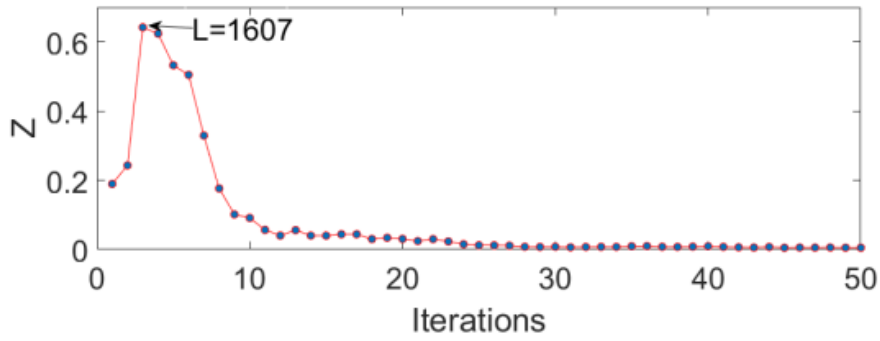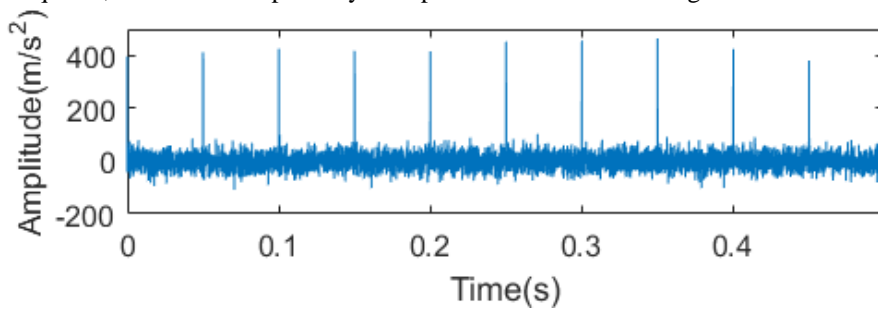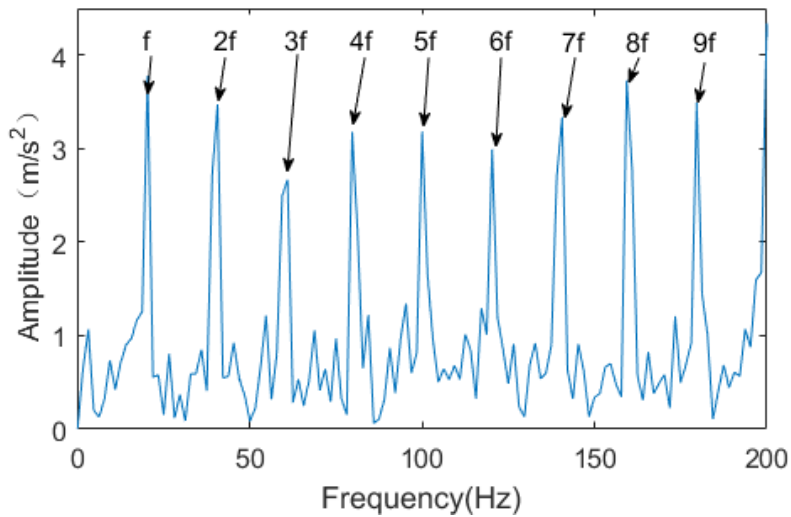Fig 20: Temporal waveform and envelope spectrum of outer ring fault

Fig 21: Curve of Z with the number of iterations (rotor imbalance)

When the period T is 640, L=1607 that we can see from Fig.21, and the window function is [1607,1], the time domain waveform is acquired, and the envelope analysis is processed as shown in Fig. 22.

(a)Time domain graph

(b) Envelope spectrum

Fig 22: Temporal waveform and envelope spectrum of rotor imbalance fault

After the original signal is handled by filtering, deconvolution and envelope the signal by setting different fault periods T and filter length L. From Fig. 20(b) and 22(b), the typical fault characteristic frequency and related multiples could be vividly achieved for the corresponding fault type identification.

Ⅴ. Conclusion

This paper proposes a fault identification method that basing on VMD with adaptive parameters and PSO-MOMEDA for resolve the difficulty of extracting fault characteristic frequency of rotor system under strong noise background. Through the combination of numerical simulation and experimental analysis, and the specific conclusions are as follows:

(1) For the problem that the fault characteristics are hardly to be extract due to noise contamination in the rotor system vibration signal acquisition process, the method of combining adaptive VMD and PSO-MOMEDA is proposed.

(2) For the parameter selection in the algorithm proposed in this paper, it is raised to take the indicator Z (Z=kurtosis/relative entropy) as the objective function to select the optimal value, which avoids manual intervention.

(3) The method is put forward in this paper can not only apply on a single fault in the rotor system, but also performed well in the diagnosis of compound faults for the rotor system.

Acknowledgements

References

[1] Yu FJ, Zhou FX, Yan BK (2016) Bearing initial fault feature extraction via sparse representation based on dictionary learning. Journal of Vibration and Shock 35:181–186

[2] Ding K., Chen JL, Su XR (2013) Development in vibration signal analysis and processing methods. Journal of Vibration Engineering 16:1–10

[3] Wang CG, Li HK, Hu SL, Hu RJ, Ren XP (2021) Weak fault feature extraction of planetary bearing based on parameter adaptive MOMEDA. Journal of Vibration Engineering 34:634–644

[4] Mcdonald GL, Zhao Q (2017) Multipoint optimal minimum entropy deconvolution and convolution fix: application to vibration fault detection. Mechanical Systems and Signal Processing 82:461–477

[5] WIGGINS R A (1978) Minimum entropy deconvolution. Geoexploration 9:21–35

[6] Mcdonald GL, Zhao Q, Zuo MJ (2012) Maximum correlated kurtosis deconvolution and application on gear tooth chip fault detection. Mechanical Systems and Signal Processing 33:237–255

[7] Mu G, Shi KP, An J, Ning P, Yan G G (2008) Signal energy method based on EMD and its application to research of low frequency oscillations. Proceedings of the CSEE 28:36–41

[8] Bie FF, Du TF, Lv FX, Pang MJ, Guo Y (2020) An Integrated Approach Based on Improved CEEMDAN and LSTM Deep Learning Neural Network for Fault Diagnosis of Reciprocating Pump. IEEE Access 10:23301–23310

[9] Smith JS (2005) The local mean decomposition and its application to EEG perception date. J. R. So. Interface 2:443–454

[10] Meng Z, Li SS (2013) Rolling bearing fault diagnosis based on improved wavelet threshold de-nosing method and HHT. Journal of Vibration and Shock 32: 205–214

[11] Guo T, Deng M. Z, Xu M (2017) An improved EMD algorithm based on particle swarm optimization and its application to fault feature extraction of bearings.Journal of Vibration and Shock 36:183–187

[12] Zhao HY, Xu M, Wang JD (2015) Local mean decomposition based on rational hermite interpolation and its application for fault diagnosis of reciprocating compressor. Journal of Mechanical Engineering 51: 83–89

[13] Wang P, Li TY, Gao XJ, Gao HH (2019) Bearing fault signal denosing method of hierarchical adaptive

wavelet threshold function. Journal of Vibration Engineering 32:549–554

[14]   Dragomiretskiy K, Zosso D (2014) Variational mode decomposition. IEEE Transactions on signal Processing 62:531–544

[15]   Yin JF, Chen XQ, Li SL, Shao L, Li J, Liu H L (2021) Signal denosing based on optimized VMD and NLM. Computer Engineering and Design 42:1135–1142

[16]   Bie FF, Horoshenkov KV, Pei JF (2019) An approach for the impact feature extraction method based on improved modal decomposition and singular value analysis. Journal of vibration and control 5:1096–1108

[17]   Tang GJ, Wang XL (2016) An incipient fault diagnosis method for rolling bearing based on improved variational mode decomposition and singular value. Journal of Vibration Measurement &Diagnosis 36:701–707

[18]   Xu YB, Cai ZY (2017) Application of variational modal decomposition and K-L divergence to bearing fault diagnosis of vibrating screens. Noise and Vibration Control 37:160–165

[19]   Cheng FB, Tang BP, Liu WY (2008) A method to suppress cross-terms of Wigner-Ville distribution and its application in fault diagnosis. Proceedings of the CSEE 191727–1731